

# Automatic Identification of Ambiguous Prostate Capsule Boundary Lines Using Shape Information and Least Squares Curve Fitting Technique

Rania Hussein  
DigiPen Institute of Technology  
Department of Computer Engineering  
Redmond, WA, 98052  
[rhusein@digipen.edu](mailto:rhusein@digipen.edu)

Frederic D. McKenzie  
Old Dominion University  
Department of Electrical and Computer  
Engineering  
Norfolk, VA, 23529  
[fmckenzi@ece.odu.edu](mailto:fmckenzi@ece.odu.edu)

## ABSTRACT

Currently there are few parameters that are used to compare the efficiency of different methods of cancerous prostate surgical removal. An accurate assessment of the percentage and depth of extra-capsular soft tissue removed with the prostate by the various surgical techniques can help surgeons with determining the appropriateness of different surgical approaches. Additionally, an objective assessment can allow a particular surgeon to compare individual performance against a standard. In order to facilitate 3D reconstruction and objective analysis and thus provide more accurate quantitation results when analyzing specimens, it is essential to automatically identify the capsule boundary that separates the prostate gland tissue from its extra-capsular tissue. However the prostate capsule is sometimes unrecognizable due to the naturally occurring intrusion of muscle and connective tissue into the prostate gland. At these regions where the capsule disappears, its contour can be arbitrarily reconstructed with the generation of a continuing contour line based on the natural shape of the prostate gland. We present an algorithm based on a least squares curve fitting technique that uses a prostate shape equation to merge previously detected capsule parts with the shape equation to produce an approximated curve that represents the prostate capsule. We have tested our algorithms using three shapes on 13 prostate slices that are cut at different locations from the apex and the results are promising.

## Keywords

prostate capsule, least squares, shape information, automatic detection

## 1. INTRODUCTION

Despite the numerous research studies in segmenting structures from medical images [Aar94, Liu97, Pra92, Ric96, and Pat00] and reconstructing a compact geometric representation of these structures, no study, to the best of our knowledge, has been done to automatically identify the complete prostate capsule in medical images.

Permission to make digital or hard copies of all or part of this work for personal or classroom use is granted without fee provided that copies are not made or distributed for profit or commercial advantage and that copies bear this notice and the full citation on the first page. To copy otherwise, or republish, to post on servers or to redistribute to lists, requires prior specific permission and/or a fee.

Copyright UNION Agency – Science Press, Plzen, Czech Republic.

As studies show, identifying the prostate capsule is essential in staging prostate cancer and it greatly affects the treatment options since the presence of metastases in the prostate's adjacent organs is highly related to the penetration through the prostate capsule, which therefore influences the prognosis after surgical and hormonal treatment [McN90]. In addition to its importance in prostate prognosis, automatically identifying the prostate capsule provides a more accurate and objective assessment of the percentage and depth of extra-capsular soft tissue removed with the prostate by the various surgical approaches. Not only does this assessment allow surgeons to compare the quality of one surgical approach versus another, it also provides an evaluation of surgeons' surgical performances as related to a standard [McK03]. Recent studies are focused more on a statistical model based segmentation algorithms [Pra92, Lor97, Gon04, Chi04, Bet05] than deformable models [Kas87, Pat98, Lad00, Kno99a, Kno99b].

By analyzing the existing literature, the error resulting from applying prostate segmentation methods may increase considerably when the image contains shadows with similar gray level and texture attached to the prostate, and/or when boundary segments are missing. Another obstacle that faces segmentation is the lack of sufficient number of training (gold) samples if a learning technique is used. Although algorithms based on active contours have been used successfully, their major drawback is that they depend on user interaction to determine the initial contour.

Therefore, a new segmentation approach should ideally possess certain properties:

- User interaction (e.g. defining seed points or manually placing initial contour) should be eliminated due to its drawbacks such as time consumption, human bias and/or error.
- Sample-based learning should be avoided because it is difficult to provide a large number of training samples in medical environments.
- Robustness of the segmentation algorithm with respect to the presence of noise and shadow is crucial.
- Shape information should be incorporated into segmentation algorithms to be able to estimate contour segments that are missing in some areas.

Our objective is to establish an algorithm which attempts to avoid the problems that exist in literature and to satisfy the above conditions as much as possible.

## **2. DETECTING PARENCHYMAL CONTOURS AND AREAS OF CAPSULE TISSUE**

In pathology, tissue samples are processed and made into stained tissue sections to be mounted on glass slides for interpretation. Representing the histological features of a slide in digital formats may require using a very high resolution capturing device that can capture the details of the tissue as seen under a microscope.

There are several successful attempts in literature to classify tissues of histopathologic images using texture analysis and image morphology [Dia04, Ham97, Ned00, and Pet04]. For example, the authors of [Pet04] were able to correctly identify the different tissue structures in H&E stained histology slides with  $89\% \pm 0.8$  accuracy. The authors were able to identify fat cells, stroma, nuclei of cells of epithelial origin, and other two types of nuclei that represent inflammatory cells and cancer cells. The slides were scanned using a 40X magnification lens, covering almost all the tissue. Accordingly, we conclude that the collagenous fibers within the prostate capsule as well as the epithelial cells can be

automatically identified using either of the techniques mentioned in Dia04] and [Pet04], given that the slides are scanned at 40X magnification. By detecting the epithelial cells, a parenchymal contour can therefore be generated. As for the tissue parts where the prostate capsule exists, the algorithms mentioned above can automatically detect them and mark them on the slices' images to be used as inputs to our algorithms which we will explain in the following sections.

## **3. ESTIMATION OF THE PROSTATE CAPSULE USING SHAPE INFORMATION**

In order to automatically identify the capsule of the prostate and replace the arduous and costly manual process of detecting it, a software algorithm was developed that recognizes the capsule utilizing elements of prostate anatomy and shape. Certain anatomical features make capsule generally detectable; however, the capsule is unrecognizable in some areas because of the naturally occurring intrusion of muscle into the prostate gland at the anterior apex and fusion of extraprostatic connective tissue with the prostate gland at its base. At these regions where the prostate capsule disappears, its contours need to be reproduced by drawing a continuing contour line from those areas where the capsule can be objectively recognized. The elastic fibers within the prostate capsule can be clearly recognized under the microscope and also under high resolution of scanned digital images. In order to correctly locate those lines, it is essential to detect the parenchymal outer contour of the prostatic glandular epithelial elements [McK03], since the capsule is normally located between this contour and the perimeter of the slice.

### **3.1 A Mathematical Model for a Standard Prostate Shape Top Down Anterior To Posterior**

In general, any prostate has a standard shape that can be defined in terms of equations as we had reported in a previous publication [Hus04]. Those equations can be approximated by the Limaçon curve equation

$$r = b + a \cos \theta$$

The limaçon serves only as an approximation since there is always a degree of roundness to this shape. Therefore, the limaçon serves as a better shape than a circle but may not be as good as an ellipse where more elongated prostate shapes are observed.

### 3.2 Approach

We present a general process that utilizes different shape algorithms to detect the prostate capsule. This process can be summarized as follows:

- Using digital images of prostate slices scanned with 40x magnification, identify the input sections of the prostate capsule (the outer perimeter, the parenchymal contour, and the observable portions of the capsule) automatically using texture analysis techniques [Dia04].
- Use the least squares shape algorithm to generate a curve that interpolates between the parts generated in step 1.
- Adjust the generated curve so that it does not violate any constraints. In our case the constraint is that the curve should be between the parenchymal contour and the prostate perimeter.
- Repeat steps 2 and 3 until a satisfactory threshold is acquired.

#### 3.2.1 The Least Squares Shape Algorithm

The least squares method is a very popular technique used to compute estimations of parameters and to find the best fitting model for discrete data. It is widely used in literature to fit a function (which may represent a certain shape) to a set of data which can be used in many applications including medical imaging [Pi196].

Assuming that we have a number  $n$  of discrete data  $(x_1, y_1), (x_2, y_2), \dots, (x_n, y_n)$  and  $f(x)$  is a function for fitting a curve. Therefore,  $f(x)$  has the deviation (error)  $d$  from each data point, i.e.  $d_1 = y_1 - f(x_1), d_2 = y_2 - f(x_2), \dots, d_n = y_n - f(x_n)$

The best-fit curve is the curve that has the minimal sum of the deviations squared from a given set of data, i.e. it is the curve that satisfies the following equation

$$\text{Minimum Least square error } (E) = d_1^2 + d_2^2 + \dots + d_n^2$$

$$= \sum_{i=1}^n d_i^2 = \sum_{i=1}^n [y_i - f(x_i)]^2$$

#### 3.2.2 Implementing the least squares using the limaçon shape equation

We have used the least square error to find the closest location of the prostate shape equation with respect to the parts of the capsule that are present in the tissue (Figure 1)

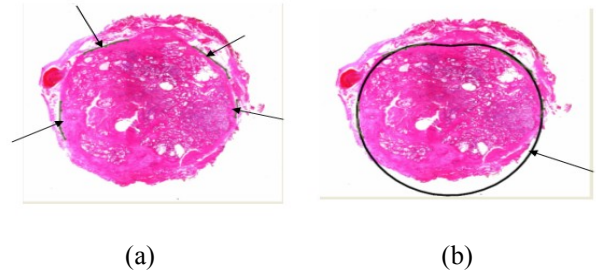


Figure 1. Least squares method and prostate shape equation. (a) Arrows point to the detected parts of the prostate capsule, (b) Arrow points to the curve representing the prostate shape located as close as possible to the capsule parts.

#### Known Capsule Regions Preservation

Once the curve is positioned close to the capsule parts, parts of the shape curve is replaced by the capsule segments and a new curve is generated by connecting all the curve points and capsule points using cubic splines (Figure 2)

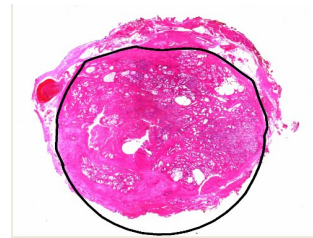


Figure 2. New shape curve after merging the capsule parts into the original shape curve.

#### Curve Adjustment Algorithm

Sometimes the generated curve violates the constraint that states that the prostate capsule is typically located between the parenchymal contour and the prostate perimeter as shown in Figure 3.

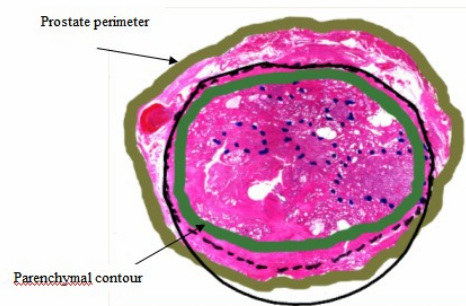


Figure 3. Shape curve extending beyond the prostate perimeter.

In this case, we use the flood fill algorithm to relocate the curve parts that violates the constraint such that new points are generated between the 2

contours (Figure 4) for the least square algorithm to be executed again for better results.

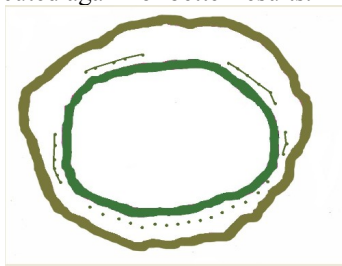


Figure 4. Contours.

The curve adjustment algorithm was used primarily to generate new boundary points to feed the shape algorithm for consecutive runs for improved shape fitting. However, in case that one wishes to stop after a certain number of runs and the output curve extends beyond the slice perimeter or inside the parenchymal contour, the algorithm is used as a final step to enforce this constraint. This enforcement may result in some sharp edges; a curve smoothing technique can be added as a future extension to our algorithm to solve this problem.

#### 4. PERFORMANCE EVALUATION

To evaluate the performance of the least squares algorithm, we have used two measurements, the root mean square error RMSE and the percentage of error, which are defined as follows:

##### Root Mean Square Error (RMSE):

Assuming that curves are represented by control points, the mean square error is the average of squared deviations. Deviations can be calculated by getting the distance from each point on the curve to the closest point on the reference curve. The root mean square error can be calculated by getting the square root of the mean square error as shown in the following equation:

$$RMS = \sqrt{\frac{\sum_{i=1}^n d_i^2}{n}}$$

Where

$n$  is the number of points in the curve

$d_i$  is the min distance from point  $i$  in the curve to the reference curve. The following figure shows the RMS error of the least squares algorithm

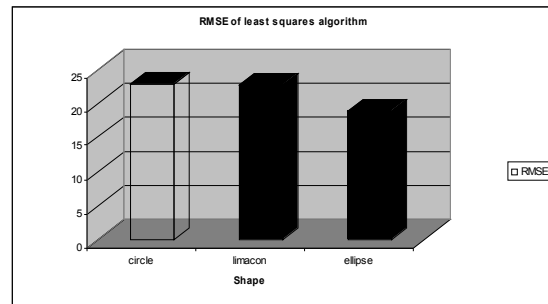


Figure 5. Root Mean Square Error for the least squares algorithm.

##### Percentage Error:

$$\text{Percentage Error} = \frac{\sum_{i=1}^m t_i}{m}$$

Where

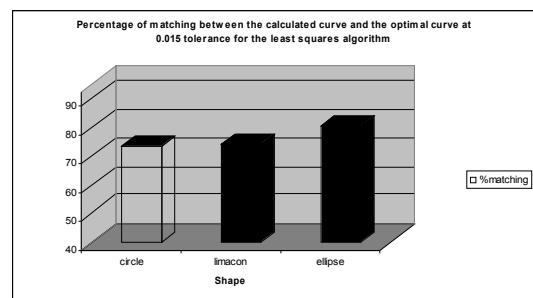
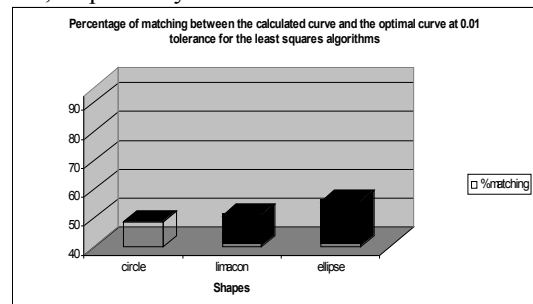
$m$  is the number of points in the reference curve

$$t_i = \begin{cases} 1 & d_i > \text{threshold} \\ 0 & d_i \leq \text{threshold} \end{cases}$$

$d_i$  is the min distance from point  $i$  in the reference curve to the curve

The thresholds considered in our study are equal to 1%, 1.5%, and 2% of the number of pixels of the image diagonal. We found that the 2% threshold, which is the biggest threshold we used, is less than 2mm in length. According to the fact that the capsule thickness is between 0.5 to 2mm [Sat95], we believe that the 2% threshold is reasonable and within acceptable limits while the 1.5% threshold is used to gauge performance improvement. The 1% result is essentially directly on top of the reference line.

The following figures show the % matching between the calculated curve and the optimal curve for the least squares algorithm at 0.01, 0.015 and 0.02 threshold, respectively.



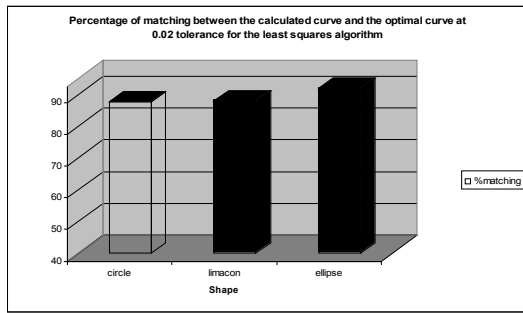


Figure 6. Percentage matching for least squares algorithm.

The results presented show the least squares shape algorithm shows an aptitude for increasing capsule detection as better shape equations are used. The results presented are the outcome of running the algorithm for 2 runs only; however, it can be run for as many times as needed until a satisfactory threshold is acquired. Obviously, increasing the number of runs for a particular specimen is more important for complex prostate equations that have more degrees of freedom.

## 5. CONCLUSION

In this paper, we presented an overall process and a novel shape algorithm to detect the prostate capsule boundary with the use of least squares fitting along with prostate shape equations. We have tested our algorithms on a data set of 13 different prostate slices and our results show promises. Our algorithm show an aptitude for increasing capsule detection as better shape equations are used.

## 6. REFERENCES

- [Aar94] R. G. Aarnik, R. J. B. Giesen, A. L. Huynen, J. J. M. C. H. De La Rosete, F.M.J. Debruyne, and H. Wijkstra, "A practical clinical method for contour determination in ultrasonographic prostate images," *Ultrasound Med Biol.* vol.20, no.7, pp. 705-717, 1994.
- [Bet05] N. Betrounia, M. Vermandela, D. Pasquierc, S. Maoucheb, and J. Rousseaua, "Segmentation of abdominal ultrasound images of the prostate using a priori information and an adapted noise filter," *Computerized Medical Imaging and Graphics*, vol. 29, pp. 43–51, 2005.
- [Chi04] B. Chiu, G.H. Freeman, M.M. Salama, A. Fenster, "Prostate segmentation algorithm using dyadic wavelet transform and discrete dynamic contour," *Phys. Med. Biol.*, vol.49, pp.4943–4960, 2004.
- [Gon04] L. Gong, S. Pathak, D. Haynor, P. Cho, and Y. Kim, "Parametric Shape Modeling Using Deformable Superellipses for Prostate Segmentation," *IEEE Transactions on Medical Imaging*, vol. 23, pp. 340-349, 2004
- [Dia04] J.Diamond, H. Anderson, P. Bartels, R. Montironi, and P. Hamilton, "The use of morphological characteristics and texture analysis in the identification of tissue composition in prostatic neoplasia," *Human Pathology* vol. 35, no. 9, pp. 1121-1131, September 2004.
- [Ham97] P.W. Hamilton, P.H. Bartels, and D. Thompson, "Automated location of dysplastic fields in colorectal histology using image texture analysis," *J. Pathol.*, vol.182, pp. 68–75, 1997.
- [Ham94] P.W. Hamilton, P.H. Bartels, and R. Montironi, "Automated histometry in quantitative prostate pathology," *Anal. Quant. Cytol. Histol.* vol. 20, pp. 443–460, 1998.
- [Hus04] R. Hussein, F. McKenzie, R. Joshi, "Automating prostate capsule contour estimation for 3D model reconstruction using shape and histological features," *SPIE-Int. Soc. Opt. Eng. Proceedings of SPIE* vol. 5367, no.1, pp.790-798, 25 May 2004, USA.
- [Kas87] M. Kass, A. Witkin, D. Terzopoulos, "Snakes: active contour models," *Int. J. Comput. Vision*, vol. 1, pp. 321-331, 1987.
- [Kno99a] C. Knoll, M. Alcaniz, V. Grau, C. Monserrat and M. Juan, "Outlining of the prostate using snakes with shape restrictions based on the wavelet transform," *Pattern Recogn.* vol. 32, no. 10, pp. 1767–1781, 1999.
- [Kno99b] C. Knoll, M. Alcaniz, C. Monserrat, V. Grau and M.C. Juan, "Multiresolution segmentation of medical images using shape-restricted snakes," *Proc. SPIE*, vol. 3661, pp. 222–233, 1999.
- [Lad00] H.M. Ladak, F. Mao, Y. Wang, D.B. Downey, D.A. Steinman and A. Fenster, "Prostate segmentation from 2D ultrasound images," *Med. Phys.*, vol. 27, pp. 1777–1788, 2000.
- [Liu97] Y.J. Liu, W.S. Ng, M.Y. Teo, and H.C. Lim, "Computerised prostate boundary estimation of ultrasound images using radial bas-relief method," *Med. Biol. Eng. Comput.*, vol.35, no.5, pp.445-454, 1997.
- [Lor97] Lorenz, C. Haas and H. Ermert, "Segmentation of ultrasonic prostate images using a probabilistic model based on markov random processes," *Ultrason. Imaging*, vol. 19, pp. 44–45, 1997.
- [McK03] F. D. McKenzie, R. Hussein, J. Seevinck, P. Schellhammer, and J. Diaz. "Prostate Gland and Extra-Capsular Tissue 3D Reconstruction and Measurement," *The 3rd IEEE symposium on Bioinformatics and Bioengineering (BIBE)*, Bethesda, Maryland, pp. 246-250, March 10-12, 2003.
- [McN90] J.E. McNeal, A. Villers, E. Redwine, F. Freiha, and T.A. Stamey, "Capsular penetration in prostate cancer: significance for natural history and treatment," *Am. J. Surg. Pathol.*, vol. 14, pp. 240-247, 1990.
- [Ned00] P. Nedzved, "Morphological Segmentation of Histology Cell Images," *IEEE ICPR'00*, vol.1, pp.1500, 2000.
- [Pat98] S. Pathak, R. Aarnink, J. de la Rosette, V. Chalana, H. Wijkstra, F. Debruyne and Y. Kim, "Quantitative three-dimensional transrectal ultrasound for prostate imaging," *Proc. SPIE*, vol. 3335, pp. 83–92, 1998.
- [Pat00] S. Pathak, D. Haynor, and Y. Kim, "Edge-guided boundary delineation in prostate ultrasound images," *IEEE Transactions on Medical Imaging*, vol.19, no.12, pp.1211-19. Publisher: IEEE, USA, Dec. 2000.
- [Pet04] S. Petushi, C. Katsinis, C. Coward, F. Garcia, and A. Tozeren, "Automated identification of microstructures on histology slides," *2nd IEEE International Symposium on Biomedical Imaging: Macro to Nano (IEEE Cat No. 04EX821)*. IEEE, vol. 1, pp. 424-471. Piscataway, NJ, USA, 2004.

- [Pil96] M. Pilu, A.W. Fitzgibbon, R.B. Fisher, "Ellipse-specific direct least-square fitting," *Proceedings. International Conference on Image Processing (Cat. No.96CH35919)*. IEEE. vol.3, pp. 599-602, New York, NY, USA, 1996.
- [Pra92] J.S. [Prater](#), W.D. [Richard](#), "Segmenting ultrasound images of the prostate using neural networks," *Ultrason. Imag.*, vol. 14, pp. 159-185, 1992.
- [Ric96] W.D. Richard, C.G. Keen, "Automated texture-based segmentation of ultrasound images of the prostate," *Computerized Medical Imaging & Graphics*, vol.20, no.3, pp.131-140. Publisher: Elsevier, UK, May-June 1996.
- [Sat95] A. Sattar, J. Noël, J. Vanderhaeghen, C. Schulman, and E. Wespes, "Prostate capsule: computerized morphometric analysis of its components," *Urology*, vol.46, no.2, pp.178-181, 1995.
- [Zhu06] Y. Zhu, S. Williams and R. Zwigelaar, "Computer technology in detection and staging of prostate carcinoma: A review," *Medical Image Analysis*, vol. 10, no. 2, pp. 178-199, April 2006.